communications earth & environment

Review article

https://doi.org/10.1038/s43247-024-01823-8

Abiotic and biotic-controlled nanomaterial formation pathways within the Earth's nanomaterial cycle

Check for updates

Michael Schindler[1] ✉, Jie Xu[2] & Michael F. Hochella Jr[3]

Nanomaterials have unique properties and play critical roles in the budget, cycling, and chemical processing of elements on Earth. An understanding of the cycling of nanomaterials can be greatly improved if the pathways of their formation are clearly recognized and understood. Here, we show that nanomaterial formation pathways mediated by aqueous fluids can be grouped into four major categories, abiotic and biotic processes coupled and decoupled from weathering processes. These can be subdivided in 18 subcategories relevant to the critical zone, and environments such as ocean hydrothermal vents and the upper mantle. Similarly, pathways in the gas phase such as volcanic fumaroles, wildfires and particle formation in the stratosphere and troposphere can be grouped into two major groups and five subcategories. In the most fundamental sense, both aqueous-fluid and gaseous pathways provide an understanding of the formation of all minerals which are inherently based on nanoscale precursors and reactions.

The Earth system is unimaginably complex due to the abundance and diversity of life (from micro- to macro-organisms) intertwined with literally millions of organic and inorganic molecules and materials composed from atoms across the periodic table. To parse the system into less entangled portions, scientists have used what has become known as Earth cycles for more than a century. As such, one can more easily follow important chemical aspects of the planet, such as individual elements (e.g., carbon, nitrogen, or phosphorus), individual Earth components (e.g. rocks, water, or nutrients), or multiple related elements/components in living/non-living subsystems (e.g., one of the many useful biogeochemical cycles). Driven by the expansion of available methods and tools for examining the Earth system, more Earth cycles are realized and components studied, as for example Earth's nanomaterial (NM) cycle more recently recognized and introduced[1]. Like all cycles, the NM cycle encompasses (at least in principle) where NM are, and how they form, are distributed, and then lost or consumed as a next generation of nano-components appear throughout the Earth system.

The reason that a NM cycle is useful for Earth science, and in fact necessary in the complete study of our planet, is because these materials behave differently than entities generally smaller (e.g., most molecules), and bigger (e.g., most minerals, and biological components such as cells, while at the same time realizing that viruses are complex organic nanoparticles, and large molecules like proteins can also be considered nanoparticles). In the mineral world, by far making up the bulk of this planet and a major part of the critical zone of the Earth, nanominerals and mineral nanoparticles are not only abundant and widespread, but it has been suggested that they have been one of the principal catalytic components of Earth throughout its history[1]. They may contain any element in the periodic table, may be atomically ordered (crystalline), disordered, or amorphous, and range in size from less than a nanometer (< 0.001 microns) up to several tens of nanometers (often in the range of 0.03 to 0.05 microns). Their properties depend, like bulk materials, on their chemical composition and atomic structure. Changing either of these, even slightly, can result in very different chemical and/or physical properties. However, for NMs, their properties also depend on their size, shape, and surface topographic features. The reason that this is important is that NMs often have dramatically different chemical and physical properties relative to their macro-mineral equivalent in the bulk state (if one even exists with the same atomic structure), that is in sizes larger than a few to several tens of nanometers in one, two, or all three dimensions. It is these property changes that not only significantly impact the Earth system in many important ways, including their distribution around the planet[1,2], but for NMs in general, have also produced the nanoscience and nanotechnology revolution in the last few decades in the medical, electronic, catalytic, and chemical fields valued at trillions of US dollars worldwide each year[3].

Formation, properties, cycling and budgets of NM's in Earth compartments (lithosphere, atmosphere and hydrosphere) have been reviewed numerous times[4,5] with these papers also focusing on specific types of NMs[6,7] and their role in a vast array of Earth and environmental processes[8].

[1]Department of Earth Sciences, University of Manitoba, Winnipeg, MB, R3T2N2, Canada. [2]School of Molecular Science, Arizona State University, Tempe, AZ, 85287, USA. [3]Department of Geosciences, Virginia Tech, Blacksburg, VA, 24060, USA. ✉e-mail: Michael.schindler@umanitoba.ca

However, this field is still in its infancy with new and often unexpected discoveries constantly reported. In addition, research challenges are great due to chemical and physical complexities of nano-processes, and the exceptionally small scales that must be navigated.

This review concerning the group recognition and current understanding of abiotic- and biotic-controlled formation pathways is to the best of our knowledge the first of its type. Pathways of NM formation can occur in highly diverse environments, for example in the presence of aqueous fluids in soils, sediments, and the biological environment therein, all the way to within the gases or magmas in volcanic systems. We will focus primarily on formation pathways of NM mediated by aqueous fluids as those occur in the Earth's critical zone (CZ). Within this zone, humans interact directly or indirectly with NMs as they impact the form and function of living and non-living things[9]. However, we will also show that pathways of NM formation similar to those observed in the CZ also occur in hydrothermal systems, as well as in gas-dominated systems such as volcanic fumaroles, wildfires, and particle formation in the stratosphere and lower troposphere. Addressing pathways of NM formation outside the CZ is important as they also play fundamental roles, for example, in the cycling of elements, the formation of ore deposits, and the radiation budget of the atmosphere.

Overall, we find that despite the complexity and wide-variations of abiotic and biotic-controlled formation pathways mediated by aqueous fluids, they can be reasonably categorized into just four general types, each embodying a few to several sub-categories. For gaseous formation pathways, we have also identified two major types representing several additional sub-categories. Finally, it should be stated that determining these nano-formation pathways in natural environments is challenging, especially in that it requires very sophisticated transmission electron microscopes with the latest analytical chemistry attachments, as well as state-of-the-art sample preparation tools.

Pathways of nanomaterial formation

All the formation pathways described below are categorized in Tables 1, 2. The great majority of inorganic NM formation in the CZ consists of clay minerals due to silicate rock weathering processes[1]. Clays are considered mineral nanoparticles, as they have nanoscale thicknesses. This is one of the key nano-related factors that give them their unique properties. However, in the weathering process, other less abundant but still critically important inorganic NMs form[1]. Pathways of NM formation that are mediated by aqueous fluids also occur in the deeper portions of Earth's crust at higher temperatures. These can be driven by alteration processes or direct precipitation from meteoric water mixed with water from hydrothermal and/or magmatic sources.

Abiotic and biotic-controlled formation pathways of NMs in aqueous fluids can be coupled or decoupled from a weathering/alteration process (categories I versus II and III versus IV; Fig. 1 and Table 1). Coupled pathways are commonly based on dissolution-precipitation processes, in which the dissolution of the parent and the precipitation of the daughter(s) are closely coupled in space and time (also called interface-coupled dissolution-precipitation reactions[10]). The key components of such a pathway are the interfacial fluid phase and the porosity in the altered part of the parent phase which facilitate the mass exchange between the interface (i.e. where the dissolution-precipitation occurs) and the bulk fluid. Supersaturations and chemical compositions of the interfacial fluid as well as surface energies and stability of potential phases control the type of daughter phases that precipitate along the interface[10,11]. Here, we consider coupling of NM-formation and dissolution process when the formation occurs in a porous alteration layer or mineral surface coating. This definition assumes that the formation of the NM can be shifted in space and time and become less relevant to the dissolution process. This approach allows us to define whether biotic-controlled formations of NMs are coupled or decoupled from associated weathering/alteration processes that may have provided the bio-community with key nutrients and energy. The biotic-controlled NM-formation is considered coupled when occurring in proximity to the "parent" dissolution sites, especially within a confined space; alternatively, the formation is considered decoupled when occurring far from the parent dissolution sites, independent of the mass transfer between the dissolving mineral surface and the bulk solution.

First generation NMs may become unstable with changes in environmental conditions, composition of the pore fluid, or degree of agglomeration as it undergoes weathering/alteration. As a consequence, a second generation of NMs may form, and their formation may again be coupled or decoupled from the dissolution of the first NM-generation (Fig. 1). An alternative pathway of the first or any consecutive NM-generation is (a) their agglomeration (or flocculation) and subsequent Ostwald ripening towards larger micrometer-size grains (note that Ostwald ripening can be also considered a dissolution-precipitation process) or (b) their attachment on the surface of a growing crystals. The latter mechanism is termed crystallization through particle attachment (CPA)[12], where the attachment of the *NM* can occur in a random or orientated fashion. For random attachment, structural re-organization is required for incorporation of the *NM* into the bulk crystal, whereas orientated attachment requires the rotation of the *NM* upon attachment[13].

A classification of abiotic-controlled pathways of nanomaterial formation in aqueous fluids (I and II)

Pathways to the NM-formation coupled with weathering/alteration processes, can be further distinguished based on whether the NM is part of a first (Ia) or second or consecutive NM-generation (Ib; Table 1). The formation of a first NM-generation coupled with a weathering/alteration process can be then further subdivided into I. those where the parent material is also a NM (*Ia1*); II. the composition of the NM is controlled by the release of a minor (*Ia2*) or major element (*Ia3*) of the parent phase; and III. multiple types of NMs form simultaneously (I*a4*). Examples of pathways are listed in Table 1.

An example for *Ia1* is the illitization of smectite to interstratified illite-smectite mixtures (I-S). Following the Ostwald step rule, the pathway from smectite to I-S and to illite involves a sequence of metastable phases that form via dissolution precipitation reactions[14,15]. This pathway is favoured by temperature and has been used as an empirical geothermometer. An environmental relevant pathway in this category would be the sulfurization of engineered or incidental Ag nanoparticles into Ag_2S NMs[16,17] as the formation of the lower soluble Ag_2S decreases the bioavailability of Ag in aquatic systems[18].

In *Ia2*, the minor element in a dissolving phase will be the major constituent of the NM whereas the major elements form a bulk material hosting the NM. The bulk material may also be composed of nano-domains[19] that have undergone partial Ostwald ripening, but for simplification purposes, are not considered NM. Pathways in this category include the alteration of Cr-rich pyroxene and Au-bearing pyrite or -arsenopyrite and the subsequent formation of clinochlore and hematite/ pyrite/arsenopyrite (bulk phases) and chromite- and gold-nanoparticles, respectively (Fig. 2a, b)[19–21]. The subsequent weathering of clinochlore results in the release of chromite nanoparticles, which appear in contrast to Cr^{3+} aqueous species less susceptible to oxidation by Mn-oxide phases towards hexavalent Cr[22]. The formation of gold nanoparticles along the pyrite-hematite interface (Fig. 2a, b) can lead to their agglomeration and formation of supergene gold deposits[20].

Environmental relevant pathways in *Ia3* include the formation of amorphous silica and ferrihydrite on the surfaces of altered feldspars/plagioclase and pyrite[23,24]. The formation of an amorphous silica-gel coating provides nucleation sites for the subsequent formation of clay minerals (see below), and the gel's reorganization (as observed for borosilicate glass) can lead to the passivation of the underlying mineral[25]. The formation of such an armouring silica-rich mineral surface coating on Ca-silicate minerals could affect the release of Ca into the ocean and thus the sequestration of CO_2[26–30]. Similarly, the formation of ferrihydrite on pyrite and its potential transformation into the more stable Fe-oxide phases goethite and hematite decreases the dissolution rate of pyrite and thus the generation of acidity in mine tailings[31]. *Ia3* also includes the common pathway where a more soluble mineral is replaced by NMs of a less soluble mineral. An example would be

Table 1 | Examples for formation mechanisms of natural and incidental nanomaterials (NMs) in fluids

I. Abiotic formation coupled in space and time with weathering and alteration			
Location or environment of weathering/alteration	**Parent**	**Daughter NM**	**Reference**
a. Formation of a first-generation NMs			
1. Formation of NM replacing a first generation of NM			
Oceanic bentonite-sediments in subduction zone; altered rhyolitic hyaloclastite	Smectite	Interstratified illite-smectite mixtures with various illite-smectite ratios	14,101
Soils, sediments	Ferrihydrite	Nano-Goethite or hematite	33
Soils, sediments and wastewater	Engineered or incidental Ag nanoparticles	Ag_2S NM	16
2. Formation of only one type of NM which contains a minor element of the parent			
Alteration of ultra-basic rocks during greenschist metamorphisms	Cr-rich pyroxenes	Clinochlore (bulk) + chromite NMs	21
Low-T alteration	Au-bearing pyrite	Au NM + hematite (bulk)	20. Figure 2a, b
Hydrothermal alteration	Au-bearing As-rich pyrite	Au NM +polycrystalline matrix of pyrite and arsenopyrite	19
3. Formation of only one type of NM which contains the major element of the parent			
Soil	K-Feldspar	"paracrystalline" phase or "gel"	23
Soil, sediment	Pyrite, Fe_2S	Ferrihydrite	24
Contaminated soils	Ag_2S	HgS	32, Fig. 2c, d
4. Syn-formation of more than one type of NM			
Pedogenic altered basaltic glass in volcanic ash (dry-cool conditions)	Volcanic glass	amorphous Si-Al-Fe-phase + ferrihydrite	33, Fig. 2e, f
Soil	Fe-rich chlorite	halloysite-kaolinite, goethite, hematite, interstratified chlorite-1:1 sheet silicate	102
b. Formation of a second or consecutive generation of NMs after the weathering/alteration of a first-generation nano-daughter phase			
1. Formation of NM via amorphous precursors			
Location or environment of weathering/alteration	Parent	Daughter NM	Reference
Soil	K-Feldspar	"protocrystalline layer" depleted in Ca, Na, K and Si, enriched in Fe → halloysite and kaolinite	34
Soil	Fe-rich pyroxene	1st Generation: amorphous Fe-Si-rich matrix → green rust 2nd generation: goethite, magnetite, jarosite, Ni-rich spinel; 3rd generation: P-rich ferrihydrite → illite +chlorite	35, Fig. 2g, f
2. Formation of chemically related NMs with the addition or removal of minor constituents from the alteration layer			
Soil, Weathering profiles	Biotite	oxybiotite → vermiculite → kaolinite + Fe/Al oxyhydroxides	36,37
Soil	Muscovite	Illite-smectite → smectite → kaolinite	34
3. Formation of chemically related NMs with the addition or removal of a major constituent from the alteration layer			
Mine tailings	Pyrite	Weak acidic to basic pH range: ferrihydrite → goethite	24,38
Groundwater	Uraninite	Si-rich uraninite → coffinite	39,40
II. Abiotic formation decoupled in space and time with weathering and alteration			
a. Heterogeneous nucleation of NMs on chemically reactive redox sites in pores or on surfaces			
Environment	Host	NM	Reference
Soils	Organic matter	Cu or Ag through reduction of $Cu^{+/2+}$ and Ag^{+} on functional groups	17,41–43
Hydrothermal	Fe-bearing phyllosilicates	Cu in interlayer, reduction by Fe^{2+}	44–48
b. Heterogeneous nucleation of NMs on sites in pores or on surfaces			

Table 1 (continued) | Examples for formation mechanisms of natural and incidental nanomaterials (NMs) in fluids

II. Abiotic formation decoupled in space and time with weathering and alteration			
Soils	Pores in organic matter	amorphous silica → Cu-Zn-bearing magnetite (Fe_3O_4), cuprite (Cu_2O) and spertiniite ($Cu(OH)_2$)	51
Soils	Pores in mineralized organic matter	Franklinite	103
Soils	Fungi	Ca-oxalate	52
Soils	Interior surface of plant	Au	55
Soils and tailings	Bacteria	clays and silica	53
Tailings	Granite	Schwertmannite	54
Various types of hydrothermal ore deposits	Pyrite, As-rich pyrite Arsenopyrite	Au, other types of sulfides, sulfarsenides	19,104,105
c. Homogeneous nucleation of NMs due to changes in pH, P, T, O_2 fugacity and activity of species			
Environment	Variables/Processes	NM	Reference
1. Low T processes			
Riverine system	pH from acidic organic rich to neutral with less organics	Ferrihydrite	58
Riparian Zone	Changes in redox conditions	Ferrihydrite	59
2. High T processes			
Black smokers	P, T and mixing with seawater	Au, Bi, sulfides tellurides	61
Black smokers	P around ascending fluids	Au	60
Epithermal ore deposits	coagulation of Au NM due to cooling/ boiling/catalysis	Au	62
III. Biotic formation coupled in space and time with weathering and alteration			
a. Formation of NMs through energy metabolisms (redox reactions) of organisms			
Environment	Parent	Daughter NM	Reference
Mineral surface coatings in soils and Quaternary sediments	hematite/jarosite	Magnetite	63, Fig. 3a
b. Formation of NMs that directly provide beneficial functions for the organism			
Environment	Parent	NM	Reference
Mineral surface coatings in soils	Jarosite	Magnetite	35, Fig. 3b, c
c. Formation of NMs involving organismal cellular components or through reactions with metabolites			
Mechanism	Parent	NM	Reference
biological mobilization and concentration of platinum-group elements within biofilms	ore grains	platinum-palladium	70
biological mobilization and concentration of gold within biofilms	gold-containing grains	Au	69, Fig. 3d, e
d. Formation of NMs within extracellular polymeric matrices			
Mechanism	Parent	NM	Reference
photochemistry-driven transformation	extracellular polymeric substances (freshwater lakes)	protein-like transparent particles	71
IV. Biotic formation decoupled in space and time with weathering and alteration			
a. Formation of NMs through energy metabolisms (redox reactions) of the organism			
Mechanism	Parent	NM	Reference
bacterial sulfur oxidation	hydrogen sulfide (from microbial sulfate reduction or hydrothermal venting)	elemental sulfur	67
Bacterial oxidation of sulfide for energy	Hydrogen sulfide	elemental sulfur	106, Fig. 3f, g
bacterial iron oxidation for energy	dissolved Fe(II)	2-line ferrihydrite, goethite, and amorphous phases	107
bacterial manganese oxidation for energy	dissolved Mn(II)	manganese (IV)/(III) oxide	108
fungal reduction of selenite	Dissolved Se	Selenium	109

Table 1 (continued) | Examples for formation mechanisms of natural and incidental nanomaterials (NMs) in fluids

IV. Biotic formation decoupled in space and time with weathering and alteration			
b. Formation of NMs that directly provide beneficial functions for the organism			
Environment	Location	NM	Reference
A range of environments where cyanobacteria thrive	intracellular biomineralization (regulating bacterial buoyancy)	calcium carbonate	68, Fig. 3h, i
Marine and freshwater	intracellular biomineralization (storing iron source)	hydrated amorphous silica	110,111
c. Formation of NMs involving organismal cellular components or through reactions with metabolites			
Environment	Parent	NM	Reference
a range of anoxic/sulfide-rich environments	Microbial-reduced sulfate species	iron sulfide (greigite, mackinawite, pyrite, and pyrrhotite)	66
Lake sediments	sedimentary sulfate	Greigite	112
Messinian Black Sea sediments	Terrigenous input of sulfate	Greigite	113
Abandoned mine	microbial reduced sulfate	Sphalerite	114
contaminated streambank soils	biological- sulfidation	Metacinnabar	74, Fig. 3j
groundwater aquifers, uranium deposits/tailings	microbially mediated reduced species (usually through iron reduction or sulfate-reduction)	Uraninite	115,116
deep sea hydrothermal vents	biologically mediated reduction/ adaptation of Hg species	Mercury	117

the replacement of Ag_2S (acanthite) by NMs composed of HgS (cinnabar) (Table 1; Fig. 2c, d)[32]. An example for Ia4 would be the simultaneous formation of a silica-rich amorphous NM and ferrihydrite during the weathering of volcanic basalt glass (Fig. 2e, f and ref. 33).

The formation of consecutive NM-generations (*Ib*) requires the formation of a first generation of NMs and is thus a subcategory of *Ia*. However, we treat *Ib* as its own as it allows for deciphering additional pathways of NM-formation. Formation of NMs of the second or consecutive generation can be further subdivided into those which form from an amorphous precursor (*Ib1*), through the addition or removal of a minor constituent from the alteration layer (*Ib2*) or to the addition or removal of a major constituent to the alteration layer (*Ib3*). As the NM-formation in these categories often requires the addition of chemical constituents from the bulk fluid, their formation is thus not entirely coupled to the weathering/alteration process of the underlying mineral.

An example for *Ib1* would be the pathways from an amorphous silica-rich precursor to consecutive generations of clay minerals on the surface of an altered feldspar[34] or the formation of different Fe-bearing NMs from an amorphous Fe-silica-rich precursor on the surface of an altered Fe-rich pyroxene (Fig. 2g, h)[35].

Pathway of *Ib2* occurs, for example, during the alteration of micas. Here the pathway is initiated with the hydration (addition of H_2O and OH groups) and oxidation of muscovite and biotite followed by the formation of multiple generations of clay minerals on their surfaces (removal of alkaline cations)[34,36,37]. Pathways of *Ib3* include for example the formation of multiple generations of Fe-hydroxides, including a first generation of nanocrystalline ferrihydrite on the surface of pyrite (i.e. removal of sulfur[24,38]) and the conversion of uraninite into a highly disordered silica-rich uraninite (addition of silica) followed by the formation of coffinite, $USiO_4$ (this process is also called coffinization of uraninite[39,40]). The latter process is common in uranium ore deposits and may also be relevant during the interaction of nuclear fuel waste (the natural analogue to uraninite) with silica-rich fluids.

Formation processes decoupled from weathering processes (II) involve the transport of released constituents from the dissolving mineral surface and alteration layer to areas of either higher reactivity or different environmental conditions.

Areas of higher reactivity can be reactive surface sites on minerals or organic material that chemically transform (oxidize or reduce) elements adsorbed to their surface (*IIa*). Reactive surface sites can be also highly underbonded surface terminations along surfaces, terraces, edges, or kink sites of organic matter, plants and minerals at which the initial adsorption of aqueous species results in the heterogeneous nucleation of NMs (*IIb*). The transport of constituents to areas of different environmental conditions such as pH, Eh, P, T often promote the homogeneous nucleation of NMs (*IIc*).

Examples for *IIa* include the diffusion of $Cu^{1+/2+}$ and Ag^{+}-bearing species into organic matter and their reduction by organic functional groups and the subsequent formation of Cu and Ag nanoparticles[17,41–43]. A similar pathway occurs when $Cu^{1+/2+}$-bearing species enter the interlayer of Fe^{2+}-bearing phyllosilicates and become reduced by Fe^{2+} terminations along the octahedra layers of the sheet silicates[44–48]. Both processes are relevant to the sequestration of Cu in smelter- and mining-impacted soils.

The heterogeneous NM-nucleation in pores or on surfaces of organic matter, minerals, bacteria, fungi and plants is often induced through the provision of a nucleation site but can be also controlled by the pore size and pore shape. For example, a decrease in pore diameter enhances the formation of inner-sphere complexes on the surfaces of the nanopores (via a decrease in the surface acidity constants of the surface functional groups) and thus leads to the accumulation of NM-constituents in the pore[49]. However, a decreasing pore size also increases the solubility of the material due to limiting its size (expressed in the Pore Controlled Solubility (PCS) model[50]). Hence, the formation of NMs in pore spaces can be based on a combination of different pathways (i.e. heterogeneous nucleation versus supersaturation) but is in this study assigned to only one category. Examples for the formation of NMs in porous materials include the formation of amorphous silica, Cu-(hydr)oxides and minerals of the spinel group (magnetite, Fe_3O_4 and franklinite, $ZnFe_2O_4$) in porous organic matter in Cu-contaminated soils[51]. The heterogeneous nucleation of NMs was observed on reactive surfaces of fungi, plants, bacteria and granite and include for example Ca-oxalate, gold, clays and schwertmannite,

Table 2 | Examples for formation mechanisms of natural and incidental NMs in the gas phase and during magmatic processes

V. Abiotic pathways of NM formation in the gas phase: thermal decomposition, volatilization, oxidation, sublimation, solidification, freezing and thermal alteration during incidental combustions			
a. High-T processes			
Environment	Variables/Processes	NM	Reference
1. Wild- and coal fires			
Soil-plant interface	Wildfires set by lightning	amorphous carbon $CaCO_3$, $FeCl_2$, $FeSO_4$ $Fe(NO_3)_3$, $FeCl_3$, magnetite	79,94
Thermal alteration aureoles along coal-sediment interface	Coal fires set through spontaneous combustion or lightning	soot, nanotubes, fullerenes, tar at high T: oxides and silicates at < 630 °C: sulfates and sulfides	80
2. Volcanic activities			
Volcanic fumaroles	Changes in T	Au	85,86,118
Volcanic eruptions	Redox reactions between silica glass and carbon monoxide	Cristobalite	84
b. Low T processes			
Environment	Process/source	NM	Reference
1. Freezing			
Troposphere to Stratosphere	Freezing	ice, crystalline acid hydrates such as $H_2SO_4{\cdot}4H_2O$, $HNO_3{\cdot}3H_2O$	75
2. New particle formation			
Lower troposphere	New particle formation through oxidation of S- and N- species and organic components from natural (e.g. volcanic eruptions) and anthropogenic sources	mascagnite, $(NH_4)_2SO_4$, critical nuclei containing sulfates, nitrates, organic matter	75,76,87
3. Sea spray			
CZ to Lower troposphere	Nucleation from sea spray, often associated with other atmospheric particles	halite, NaCl, gypsum, $CaSO_4{\cdot}2H_2O$, glauberite, $Na_2Ca(SO_4)_2$, loweite, $Na_{12}Mg_7(SO_4)_{13}$	77
VI. Pathways of NM formation during magmatic processes			
Host/environment	Processes	NM	References
pyrrhotite, millerite, pyrite, pentlandite and chalcopyrite in mafic-ultramafic Rocks	Changes in T, fO_2 and activity of sulfide and silica	PGE-alloys, -sulfides, -tellurides, -stannides	96,98,119–121

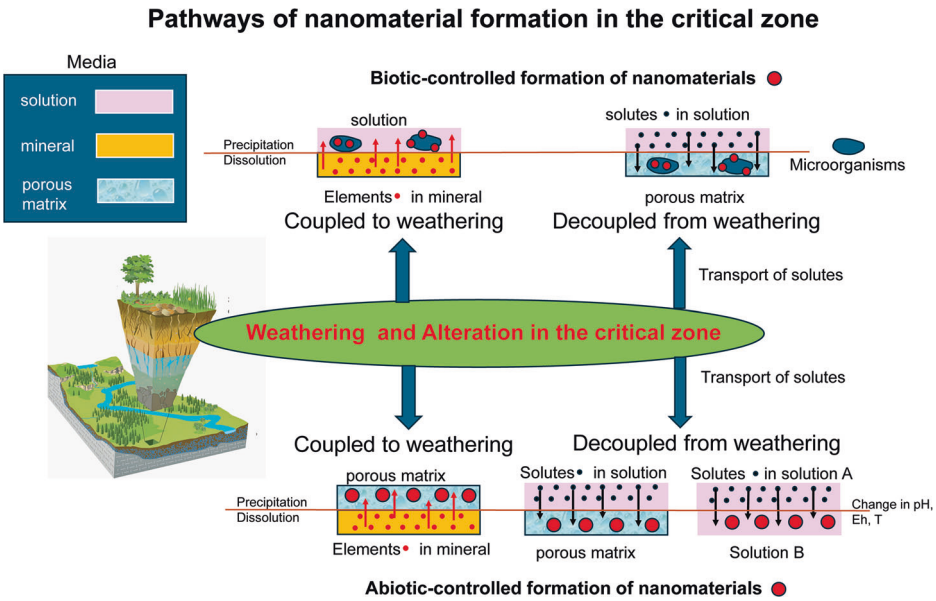

Fig. 1 | Schematic overview of various pathways of nanomaterial formation in aqueous fluids within the critical zone (the sketch of the critical zone is adapted from[122]). The upper half of the schematic is for biotic-controlled pathways, and the lower half for abiotic-controlled pathways; brown-coloured lines indicate interfaces between solution-porous matrix, solution-mineral and between solutions of different compositions and environmental conditions (indicated as changes in pH, Eh and T (temperature); the different types of media are listed in the upper left corner and are depicted in the schematics of the pathways in pink (solution), orange (minerals) and light blue (porous matrix), in the latter schematics, nanomaterials are shown as large red circles, elements in minerals as small red-coloured circles, solutes in solution as small black circles and microorganisms as blue-coloured oval-shaped forms.

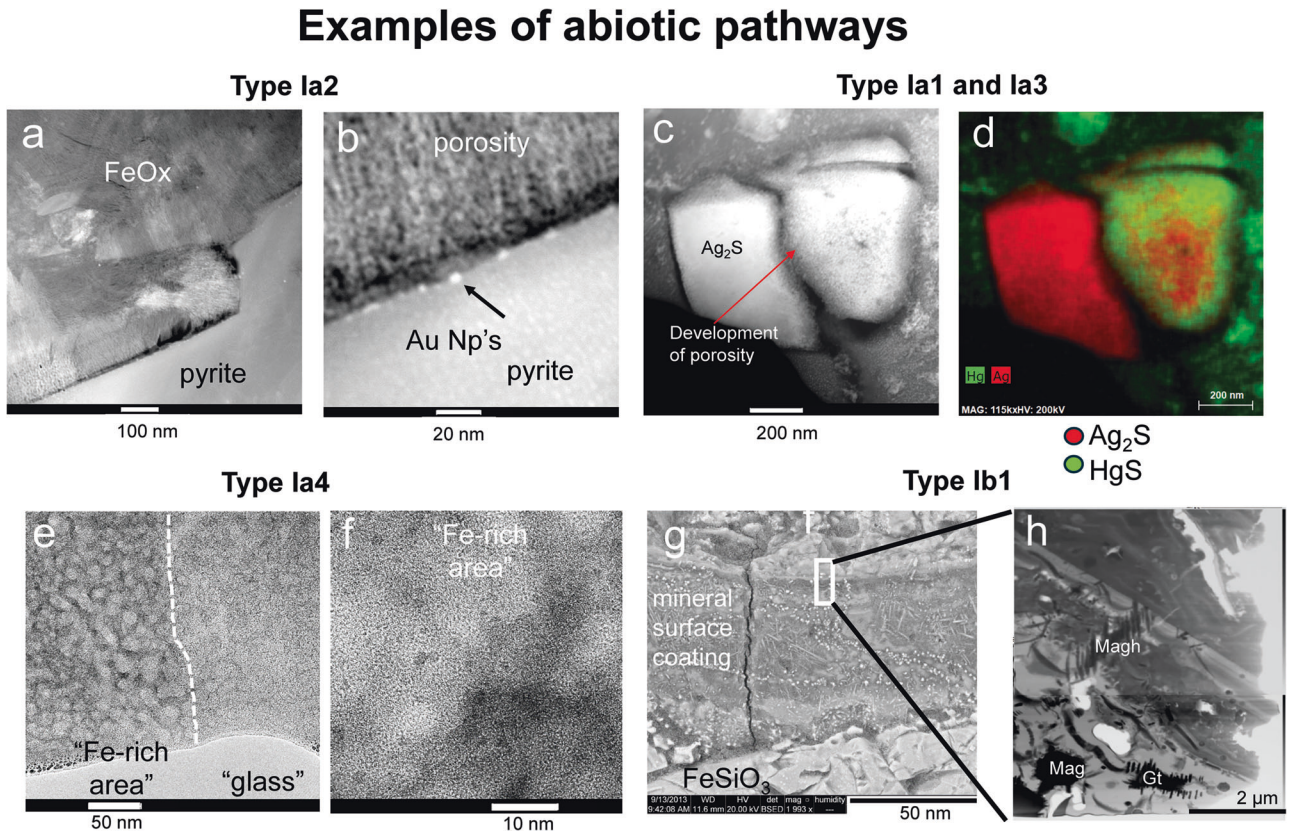

Fig. 2 | Examples of abiotic pathways of nanomaterial (NM) formation. **a**, **b** Example for pathway *Ia2*: Scanning-TEM (STEM) images of the formation of gold nanoparticles (Au NP's) along the interface of pyrite and Fe-oxides (Fe-Ox). **c**, **d** Example for pathway I*a3* (and for *Ia1* if the Ag_2S grains are considered to be nano in size): (**c**) STEM image and (**d**) STEM-EDS chemical distribution map for Ag (red) and Hg (green) indicating the replacement of a Ag_2S grain (on the right) by HgS (green rim)[32], **e**, **f** Example for pathway *Ia4*: TEM images of the simultaneous formation of ferrihydrite and amorphous silica NM during the weathering of volcanic glass[33]; (**e**) overview image depicting areas with high ("Fe-rich area") and low ("glass") degree of weathering; (**f**) higher magnification image of individual ferrihydrite particles (in the lower nanometer-size range) embedded in an amorphous silica matrix. **g**, **h** Example for pathway Ib1: SEM-BSE image of a part of a mineral surface coating on a Fe-rich pyroxene and TEM image depicting numerous Fe-(hydr)oxide formed in the matrix of an amorphous Fe-silica phase[35], the area depicted in (**h**) is indicated with a white square in (**g**); (**a**, **b**, **e**–**h**) are unpublished images from features previously shown in[20,33,35]; the different types of pathways are indicated with the codes "Iax" or "Ibx" with x = 1, 2, 3 and 4; "I" indicates the main category, "a" and "b" subcategories and "1, 2, 3 and 4" additional subcategories (see text and Table 1 for details); (**c**, **d**) are reproduced with permission from the Royal Society of Chemistry.

respectively (Table 1)[52–55]. Under hydrothermal conditions, Au and sulfide-NMs often nucleate on the surfaces of pyrite or As-rich pyrite and occur within growth zones of these minerals[19].

Many pathways exist for the homogeneous NM-nucleation due to changes in environmental conditions[34,56,57] (IIc). One important pathway affecting the transport of the nutrient Fe to the ocean is the formation of ferrihydrite in riverine or riparian zones due to changes in pH and Eh, respectively[58,59].

An important ore forming process is the pathway from dissolved metals in hydrothermal fluids to sulfate, sulfide and native element NMs around black smokers[60,61] and in hydrothermal veins[62]. The pathway of their formation is initiated by the boiling of the hydrothermal fluids due to a decrease in pressure, the mixing of the fluids, and the loss of reducing gases such as H_2S and H_2 which subsequently result in the oxidation of redox-sensitive ions, an increase in the respective saturation indices, and homogeneous NM-nucleation.

A classification of biotic-controlled pathways of NM formation in aqueous fluids

The presence of naturally occurring NMs may play important, if not essential, roles in enabling and sustaining microbial metabolisms. Living organisms may be involved in the NM formation through three ways: (1) directly utilizing a substrate (as an energy or nutrient source) and transform it into NMs (categories IIIa and IVa, Table 1); (2) actively control NM formation using their biomolecular toolbox (IIIb and IVb, Table 1); and (3) passively cause NM formation through discharging metabolites into their immediate surroundings and through the presence of their cell surfaces and extracellular polymeric substances (EPS) (IIIc, IIId, and IVc, Table 1).

Most biotic NM-formations are considered decoupled (IVa, b, and c, Table 1) unless the substrate fueling the biological growth and subsequent NM formation is trackable or physically restricted within the biological communities responsible for the NM formation (IIIa, b, c, and d, Table 1). The coupled scenarios include bio-utilization of solid-phase substrate (IIIa and b, Fig. 3) and NM formation within a confined space mediated by biological metabolisms, e.g., biofilms in the proximity to where the substrate is mobilized (IIIc, Fig. 3). It is noted that the biotic NMs in IIIa versus IIIb (Fig. 3), despite their mineralogical similarities, may reflect distinctive formation processes based on their morphologies and size distributions. The former (IIIa) was likely a result of microbial reduction of pre-existing Fe(III) phases[63] whereas the latter likely involved actively controlled intracellular biomineralization[64].

The biotic NMs formed through active biomineralization more likely behave as functional and flexible "nano tools" that may assist the biological cells or community with electron transfer, chemotaxis, and substrate storage[65]. In these cases (IIIb and IVb, Table 1), the cells precisely control of the NMs size, crystal structure, and stability through involving proteins, nucleic acids, and other biomolecules. For example, magnetite/greigite inclusions in magnetotactic bacteria as nano-compasses[66], elemental

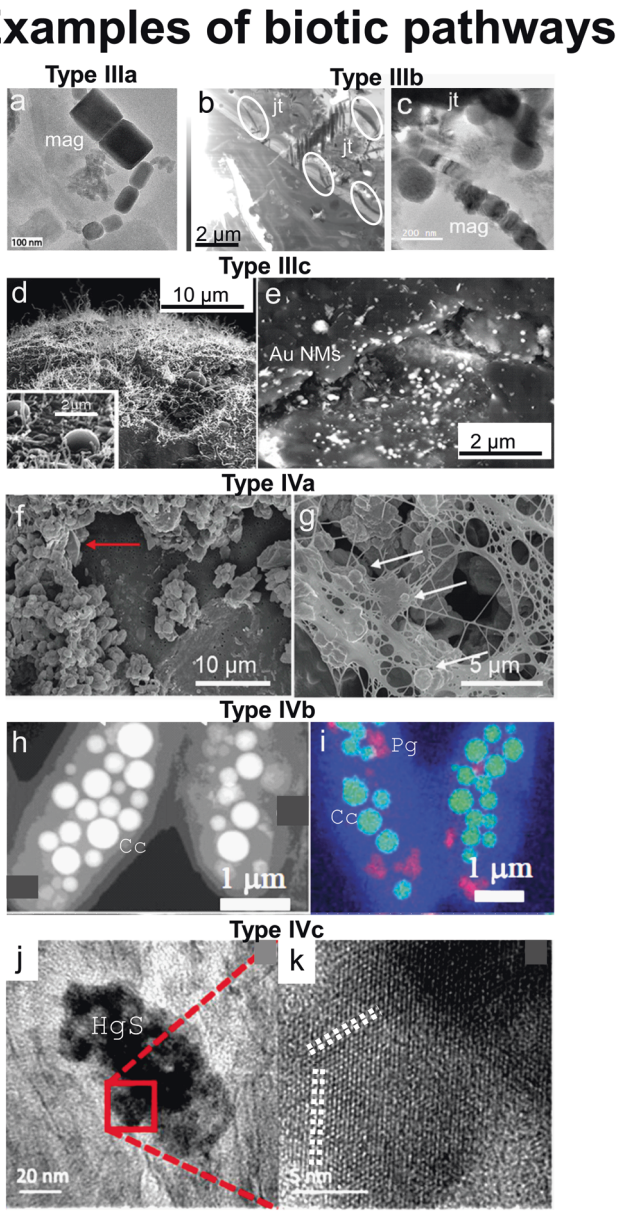

Fig. 3 | Examples of biotic pathways of nanomaterial (NM) formation. a Example for pathway IIIa: transmission electron micrographs (TEM) of magnetite (mag) NMs formed via microbial alteration of hematite[63]. **b**, **c** Example for pathways IIIb: (**b**) scanning TEM image of a focused ion beam section extracted from a soil sample obtained near a smelting center in Ontario, Canada; occurrences of petrified spirilla with the same orientation on the surface of jarosite (jt) are encircled; (**c**) TEM image of biogenic magnetite (mag) NMs in close proximity to one of the spirilla encircled in (**b**)[35]; (**d**, **e**) example for pathway IIIc: scanning electron micrographs (SEM) of gold (Au) NMs in biofilms through biological alteration of gold-containing ores[69]; the area shown in (**e**) is outlined with a white rectangle in (**d**), (**f**, **g**) example for pathway IVa: SEM images of elemental sulfur NMs formed in Sulfurovum-dominated streamer biofilms in the Frasassi Cave, Italy[106]; the occurrence of bipyramidal S(0) crystals and S(0) spheroids are indicated with red and white arrows in (**f**, **g**), respectively; (**h**, **i**) example for pathways IVb: (**h**) STEM images and (**i**) STEM-EDS chemical distribution maps for NMs of calcium carbonate (Cc, green) and Polyp granules (PG, red) formed inside cyanobacteria[68]; (**j**, **k**) example for pathway IVc: (**j**) TEM and (**k**) high-resolution TEM image of metacinnabar (HgS) NMs formed in sulfidic niches of contaminated streambank soil[74]; the HgS NMs are composed of (**j**) clusters with (**k**) domains depicting lattice fringes of different orientation (highlighted with white dashed lines); the area shown in (**k**) is highlighted with a red square in (**j**); the different types of pathways are indicated with the codes "IIIy" or "IVy" with y = a, b and c; "III" and "IV" indicate main categories and "a", "b" and "c" subcategories (see text and Table 1 for details); (**a**, **d**, **e**) are reproduced with permission from Elsevier, (**b**, **c**) from the Geological Society of America, (**f**, **g**) from Frontiers, (**h**, **i**) from the Proceedings of the National Academy of Sciences and (**j**, **k**) from the Royal Society of Chemistry.

sulphur inclusions in sulfur-oxidizing microbes as nano-stockpiles[67] (although the sulfur NM formation is also a result of direct energy metabolism), and nano-carbonate inclusions in cyanobacteria that likely regulate the cells buoyancy[68] (Fig. 3h, i), all belong to the active biotic NM-formation category. Except for the cases where organisms use pre-existing phases restricted in their mass transfer within a confined space (e.g., Fig. 3b, c), most functional biogenic NMs are considered decoupled (IVb).

In comparison to active biotic NM-formation, it is more common to find their passive counterparts in nature. Passive biotic NM formation occurs simply due to the adsorption, reduction, and concentrating effects of the cell surfaces and EPS matrices, or due to metabolite (i.e., carbonate, sulfide, and ferric iron species etc.) accumulation in the biological microenvironments. In these cases, purposely biomolecular control of the NM-formation has not been identified (IIIc, IVc, and IIId). The passive formations that involve nucleation/condensation from dissolved species are considered decoupled processes in terms of NM-evolution, and those in which the mobility of precursor phases is restricted (e.g., in biofilms, Fig. 3d, e)[69,70] are considered coupled processes. If the NM-formation involves toxic heavy metals, these processes may help to detoxify the living organisms' immediate surrounding environment (Fig. 3j). Biological EPS matrices may facilitate new exopolymer NM formation out of the pre-existing polymeric components (IIId, Table 1)[71]. They may also concentrate mobile metal species through chelation and biosorption[72,73], which occasionally lead to NM formation[74,75]. We note that the category IVc in Table 1 is inclusive of decoupled, EPS-mediated NM formation processes as naturally occurring microbial communities, by default, exist as biofilms with EPS matrices. Although EPS of biological flocculates have been previously reported as effective traps and stabilizers for pre-existing, mostly engineered nanoparticles in the environment, the focus of this paper is on the formation pathways of naturally occurring NMs, and thus we will not elaborate on this aspect.

A classification of abiotic-controlled pathways of nanomaterial formation in gases (V)

The majority of particles formed in gases occur in the atmosphere. Their sizes ranges from 1 nm to 100 µm with coarser particles originating from sea spray and volcanic activities and finer particles from combustion and particle formation via gas-to-particle conversions[76]. All these processes result in the formation of NMs, which often occur in a higher number than their micrometer-size counterparts.

Similar to pathways mediated by aqueous fluids, the formation of NM in gases can include alteration of a first generation of NM or bulk materials as well as the heterogeneous and homogeneous nucleation[77,78]. Because the role of surfaces for the formation of NM from gases is less explored in the geoscience literature relative to those in soils, sediments and aqueous fluids, we group the pathways of NM formation in gases on the basis of their ambient temperature (Va and Vb Table 2).

High-T pathways of NM formation in gases occur during incidental combustion of plants (wildfires)[79] and coal (coal combustion)[80] (Va1, Table 2), and also during volcanic eruptions and within and in the vicinity of volcanic fumaroles (Va2). The pathways of NM formation during wildfires and coal combustion are complex and generally not well understood. They are strongly temperature dependent and occur via the thermal decomposition and volatilization of the C-based material, the release of metals and volatile elements such as H, N, O, S, Cl and Se, and the alteration of soil/sediment constituents. For example, NM composed of soot, nanotubes, fullerenes and tar form during (or shortly after) the combustion process, S-, N-, Cl- and Se-bearing phases during sublimation and solidification of hot

gasses and liquids, and oxides during thermal alteration of hydroxides, clay minerals and carbonates (Table 2)[81–83].

Pathways of NM in gases during volcanic activities (Va2) include processes during eruptions and fumarolic activities. During eruptions, silica can be reduced by carbon monoxide to SiO and subsequently oxidized resulting in the nucleation of cristobalite NM[84]. Volcanic fumaroles are known to deposit minerals on surfaces of rocks and sediments such as native sulfur. Among these phases, nanoparticles of gold were identified at numerous locations[85,86].

Low-T NM pathways in gases (Vb) occur in stratosphere, troposphere and critical zone environments. In the troposphere and stratosphere, the freezing of water-containing HNO_3 and H_2SO_4 leads to the formation of ice and crystalline acid hydrates such as $H_2SO_4 \cdot 4H_2O$ and $HNO_3 \cdot 3H_2O$, an important process during annual polar ozone depletion[75]. In the troposphere, emitted volatile gases from the biosphere, volcanic activities and anthroposphere such as SO_2, NH_3, or volatile organic compounds are oxidized to low volatile trace vapors through atmospheric oxidation, a process commonly referred to as new particle formation[87]. This process leads first to the formation of molecular clusters and subsequently to the nucleation and growth of larger aerosols[88], which are defined as liquid or solid particles suspended in a gas phase. Aerosol particles influence global climate change[89] and impact human health[90]. In the upper CZ and lower troposphere, the formation of salt NM from sea spray occurs through heterogeneous and homogeneous nucleation from a fluid-gas mixture and results predominantly in the formation of halite (NaCl), gypsum ($CaSO_4(H_2O)_2$) and other sulfates (Table 2)[77].

The formation of NMs in the gas phase often has an impact on human health. For example, the TiO_2 phases rutile, anatase and brookite transform into toxic O-deficient Ti_xO_{2x-1} Magnéli phases during coal combustion. The phases occur as NMs (tens to hundreds of nm in diameter) and are significant air pollutants in regions where coal fire plants contribute to PM[91,92]. Furthermore, the formation of NMs during the recent high frequencies and sizes of wildfires (e.g., 3.8 million hectares burned in the western USA in 2020) resulted in airborne NMs (as a part of fine particulate matter, diameter ≤ 2.5 μm; $PM_{2.5}$) which (a) have the ability to penetrate deep into lungs[93], (b) can contain harmful metals from anthropogenic sources (construction and automotive)[94] and (c) can mix with other atmospheric pollutants and NM formed during low T pathways[77]. Health studies have shown that wildfire $PM_{2.5}$ is more harmful than $PM_{2.5}$ emitted from many urban environments[95].

A classification of abiotic-controlled pathways of nanomaterial formation in magmas (VI)

Pathways of NM formation during magmatic processes are commonly controlled through changes in temperature, O_2-fugacity, silica- or sulfide-activity. An economically important process is the formation of platinum group element (PGE) NMs in mafic or ultramafic sulfide- or silicate-melts[78] (Table 2). The pathway of their formation resembles those of category Ib, where minor elements in a mineral form NMs upon weathering/alteration of their original host. Field observations and experimental studies suggest that the highly siderophile and chalcophile PGEs segregate from mafic or ultramafic magmas initially into metal-rich immiscible melts (containing O, S, As, Te and Bi), followed by the formation of clusters and PGE-bearing NMs. The PGE-bearing NMs are commonly associated with ultra-mafic minerals such as chromite, pentlandite, chalcopyrite and pyrrhotite[96–98].

Overall assessment of Earth NM formation pathways

This assessment shows that the formation of nanomaterials mediated by aqueous fluids within the critical zone, as well as in many other Earth environments, follow four principal pathways which can be further subdivided into 10 abiotic and 6 biotic pathways (Table 1). Among these pathways, the most common are very likely those occurring in soils and regoliths (keeping in mind that nanomaterial formation in the oceans has not been thoroughly explored). From an economic viewpoint however, the role of NMs in the formation of ore deposits is especially intriguing as these nanoparticles provide an explanation for the transport of elements of low solubility such as Au in hydrothermal solutions[99]. In this regard, Au NM can form via five different pathways, ranging from abiotic and biotic pathways in an aqueous fluid to depositions during volcanic fumarole activity (Tables 1 and 2). This high number of pathways is most likely due to Au's low solubility and low compatibility with the structure of pyrite (i.e. which depends on T and the amount of As in the mineral).

Also, of great interest is the fact that the classification of inorganic- and organic-based pathways for NM formation based on factors such as multiple generations, amorphous precursors, energy resources, and heterogeneous and homogeneous nucleation now allow for comparisons of NM formations pathways that occur in very different chemical and physical environments. These include comparisons between NM formations during the weathering of silicates versus sulfides or between those in soils versus hydrothermal solutions. Hence, this formation pathway compilation allows for future studies by other researchers to identify formation pathways of NM similar to those observed in this study, even though the formation environment is not necessarily in geologic environments discussed in this paper. An example of this is the recent observation that the alteration of Cd-bearing sphalerite (ZnS) leads to the formation of greenockite (CdS) NMs[100]. This example follows the same pathway as the formation of gold NMs during the alteration of Au-bearing pyrite[19,20], chromite NMs during the alteration of Cr-rich pyroxenes[21], rutile NMs formed during the alteration of Ti-bearing quartz, and platinum group element (PGE) NMs formed during the alteration of PGE-bearing chromite[78].

Finally, as mentioned above, the discovery and delineation of all of the chemical/physical/biological-based pathways of NM formation in both aqueous and gaseous mediated systems will result in a better understanding of the NM cycle of the Earth as a fully connected and evolving system[1]. There is also the possibility (likelihood) that completely new and/or novel NM formation pathways will be discovered. Such conceptual frameworks have been shown repeatedly to have great value, e.g. the rock cycle, the water cycle, and the many chemical cycles of the Earth. Ultimately, the nanoreactants that appear through this cycle, including those NMs that only exist for very short times, consequently impact the entire Earth system (atmosphere, hydrosphere, and terrestrial Earth) in highly consequential ways as has been recently reviewed[1].

Methods

Features of nanomaterials published in previous studies are shown in this review. These TEM images and STEM-EDS chemical distribution maps were processed with the TEM Imaging & Analysis (a trademark of FEI) and Esprit 1 (a trademark of Bruker Nano) software.

Received: 1 May 2024; Accepted: 22 October 2024;
Published online: 01 November 2024

References

1. Hochella, M. F., Jr. et al. Natural, incidental, and engineered nanomaterials and their impacts on the Earth system. *Science* **363**, https://doi.org/10.1126/science.aau8299 (2019).
2. Hochella, M., Aruguete, D., Kim, B. & Elwood Madden, A. in *Naturally occurring inorganic nanoparticles: General assessment and a global budget for one of earth's last unexplored major geochemical components* (ed In: Nature's Nanostructures) 1-42 ((A. S. Barnard, H. Guo, Eds.) Pan Stanford Publishing, Singapore., 2012).
3. Malik, S., Muhammad, K. & Waheed, Y. Nanotechnology: A Revolution in Modern Industry. *Molecules* **28**, https://doi.org/10.3390/molecules28020661 (2023).
4. Banfield, J. F. & Zhang, H. Nanoparticles in the Environment. *Rev. Mineral. Geochem.* **44**, 1–58 (2001).
5. Ju, Y. et al. Nanoparticles in the Earth surface systems and their effects on the environment and resource. *Gondwana Res.* **110**, 370–392 (2022).

6. Guo, H. & Barnard, A. S. Naturally occurring iron oxide nanoparticles: morphology, surface chemistry and environmental stability. *J. Mater. Chem. A* **1**, 27–42 (2013).
7. Wilson, M. J. The origin and formation of clay minerals in soils: past, present and future perspectives. *Clay Miner.* **34**, 7–25 (1999).
8. Waychunas, G. A., Kim, C. S. & Banfield, J. F. Nanoparticulate Iron Oxide Minerals in Soils and Sediments: Unique Properties and Contaminant Scavenging Mechanisms. *J. Nanopart. Res.* **7**, 409–433 (2005).
9. Hochella, M. F. et al. Nanominerals, Mineral Nanoparticles, and Earth Systems. *Science* **319**, 1631–1635 (2008).
10. Putnis, A. Mineral Replacement Reactions. *Rev. Mineral. Geochem.* **70**, 87–124 (2009).
11. Navrotsky, A., Ma, C., Lilova, K. & Birkner, N. Nanophase Transition Metal Oxides Show Large Thermodynamically Driven Shifts in Oxidation-Reduction Equilibria. *Science* **330**, 199–201 (2010).
12. De Yoreo, J. J. et al. CRYSTAL GROWTH. Crystallization by particle attachment in synthetic, biogenic, and geologic environments. *Science* **349**, aaa6760 (2015).
13. Zhang, H., De Yoreo, J. J. & Banfield, J. F. A Unified Description of Attachment-Based Crystal Growth. *ACS Nano* **8**, 6526–6530 (2014).
14. Bauluz, B., Peacor, D. R. & Ylagan, R. F. Transmission electron microscopy study of smectite illitization during hydrothermal alteration of a rhyolitic hyaloclastite from Ponza, Italy. *Clays Clay Miner.* **50**, 157–173 (2002).
15. Srodon, J. Nature of Mixed-Layer Clays and Mechanisms of their Formation and Alteration. *Annu. Rev. Earth Planet. Sci.* **27**, 19–53 (2003).
16. Zuykov, M. et al. Periostracum of bivalve mollusk shells for sampling engineered metal nanoparticles: A case study of silver-based nanoparticles in Canada's experimental lake. *Chemosphere* **303**, 134912 (2022).
17. Akbari Alavijeh, M. et al. Nanoscale characterization of the sequestration and transformation of silver and arsenic in soil organic matter using atom probe tomography and transmission electron microscopy. *Environ. Sci.: Process. Impacts* **25**, 577–593 (2023).
18. Lowry, G. V., Gregory, K. B., Apte, S. C. & Lead, J. R. Transformations of Nanomaterials in the Environment. *Environ. Sci. Technol.* **46**, 6893–6899 (2012).
19. Palenik, C. S. et al. "Invisible„ gold revealed: Direct imaging of gold nanoparticles in a Carlin-type deposit. *Am. Mineralogist* **89**, 1359–1366 (2004).
20. Hastie, E. C. G., Schindler, M., Kontak, D. J. & Lafrance, B. Transport and coarsening of gold nanoparticles in an orogenic deposit by dissolution–reprecipitation and Ostwald ripening. *Commun. Earth Environ.* **2**, 57 (2021).
21. Schindler, M., Berti, D. & Hochella, M. Previously unknown mineral-nanomineral relationships with important environmental consequences: The case of chromium release from dissolving silicate minerals. *Am. Mineralogist* **102**, 2142–2145 (2017).
22. McClenaghan, N. W. & Schindler, M. Release of chromite nanoparticles and their alteration in the presence of Mn-oxides. *Am. Mineralogist* **107**, 642–653 (2022).
23. Romero, R., Robert, M., Elsass, F. & Garcia, C. Evidence by transmission electron microscopy of weathering microsystems in soils developed from crystalline rocks. *Clay Miner.* **27**, 21–33 (1992).
24. Gu, X., Heaney, P. J., Reis, F. & Brantley, S. L. Deep abiotic weathering of pyrite. *Science* **370**, https://doi.org/10.1126/science.abb8092 (2020).
25. Gin, S. et al. Dynamics of self-reorganization explains passivation of silicate glasses. *Nat. Commun.* **9**, 2169 (2018).
26. Berner, R. A. & Maasch, K. A. Chemical weathering and controls on atmospheric O2 and CO2: Fundamental principles were enunciated by J. J. Ebelmen in 1845. *Geochimica et Cosmochimica Acta* **60**, 1633–1637 (1996).
27. Dixon, J. L. & von Blanckenburg, F. Soils as pacemakers and limiters of global silicate weathering. *Comptes Rendus Geosci.* **344**, 597–609 (2012).
28. Eiriksdottir, E. S., Gislason, S. R. & Oelkers, E. H. Direct evidence of the feedback between climate and nutrient, major, and trace element transport to the oceans. *Geochimica et. Cosmochimica Acta* **166**, 249–266 (2015).
29. Frings, P. J. & Buss, H. L. The Central Role of Weathering in the Geosciences. *Elements* **15**, 229–234 (2019).
30. Hellmann, R. et al. Unifying natural and laboratory chemical weathering with interfacial dissolution–reprecipitation: A study based on the nanometer-scale chemistry of fluid–silicate interfaces. *Chem. Geol.* **294-295**, 203–216 (2012).
31. Huminicki, D. M. C. & Rimstidt, J. D. Iron oxyhydroxide coating of pyrite for acid mine drainage control. *Appl. Geochem.* **24**, 1626–1634 (2009).
32. Schindler, M., Loria, A., Ramos-Arroyoc, Y. R. & Wang, F. Nano-mineral assemblages in mercury- and silver-contaminated soils: records of sequestration, transformation, and release of mercury- and silver-bearing nanoparticles. *Environ. Sci.: Process. Impacts* **26**, 483–498 (2023).
33. Schindler, M., Michel, S., Batcheldor, D. & Hochella, M. F. A nanoscale study of the formation of Fe-(hydr)oxides in a volcanic regolith: Implications for the understanding of soil forming processes on Earth and Mars. *Geochimica et. Cosmochimica Acta* **264**, 43–66 (2019).
34. Banfield, J. F. & Eggleton, R. A. Analytical Transmission Electron Microscope Studies of Plagioclase, Muscovite, and K-Feldspar Weathering. *Clays Clay Miner.* **38**, 77–89 (1990).
35. Schindler, M. & Hochella, M. F. Jr Soil memory in mineral surface coatings: Environmental processes recorded at the nanoscale. *Geology* **43**, 415–418 (2015).
36. Dong, H., Peacor, D. R. & Murphy, S. F. TEM study of progressive alteration of igneous biotite to kaolinite throughout a weathered soil profile. *Geochimica et. Cosmochimica Acta* **62**, 1881–1887 (1998).
37. Jeong, G. & Kim, H. Mineralogy, chemistry, and formation of oxidized biotite in the weathering profile of granitic rocks. *Am. Mineralogist* **88**, 352–364 (2003).
38. Petrunic, B. M., Al, T. A., Weaver, L. & Hall, D. Identification and characterization of secondary minerals formed in tungsten mine tailings using transmission electron microscopy. *Appl. Geochem.* **24**, 2222–2233 (2009).
39. Fayek, M., Utsunomiya, S., Ewing, R. C., Riciputi, L. R. & Jensen, K. A. Oxygen isotopic composition of nano-scale uraninite at the Oklo-Okélobondo natural fission reactors, Gabon. **88**, 1583-1590 https://doi.org/10.2138/am-2003-1021 (2003).
40. Evins, L. Z. & Jensen, K. *Review of spatial relations between uraninite and coffinite - Implications for alteration mechanisms*. Vol. 1475 (2011).
41. Lovering, T. S. Organic precipitation of metallic copper: Chapter C in Contributions to economic geology (short papers and preliminary reports), 1927: Part I - Metals and nonmetals except fuels. Report No. 795C, 45-52 (Washington, D.C., 1927).
42. Fulda, B., Voegelin, A., Ehlert, K. & Kretzschmar, R. Redox transformation, solid phase speciation and solution dynamics of copper during soil reduction and reoxidation as affected by sulfate availability. *Geochimica et. Cosmochimica Acta* **123**, 385–402 (2013).
43. Mantha, H., Schindler, M. & Hochella, M. F. Occurrence and formation of incidental metallic Cu and CuS nanoparticles in organic-rich contaminated surface soils in Timmins, Ontario. *Environ. Sci.: Nano* **6**, 163–179 (2019).
44. Ilton, E. S. & Veblen, D. R. Copper inclusions in sheet silicates from porphyry Cu deposits. *Nature* **334**, 516–518 (1988).

45. Ilton, E. S. & Veblen, D. R. Origin and mode of copper enrichment in biotite from rocks associated with porphyry copper deposits; a transmission electron microscopy investigation. *Economic Geol.* **88**, 885–900 (1993).
46. IltonEugene, S., EarleyDrummondli, I., MarozasDianne, C. & VeblenDavid, R. Reaction of some trioctahedral micas with copper sulfate solutions at 25 degrees C and 1 atmosphere; an electron microprobe and TEM investigation. *Economic Geol. Bull. Soc. Economic Geologists* **87**, 1813–1829 (1992).
47. Markl, G. & Bucher, K. Reduction of Cu (super 2+) in mine waters by hydrolysis of ferrous sheet silicates. *Eur. J. Mineral.* **9**, 1227–1235 (1997).
48. Suárez, S., Nieto, F., Velasco, F. & Martín, F. J. Serpentine and chlorite as effective Ni-Cu sinks during weathering of the Aguablanca sulphide deposit (SW Spain). TEM evidence for metal-retention mechanisms in sheet silicates. *Eur. J. Mineral.* **23**, 179–196 (2011).
49. Wang, Y., Bryan, C., Xu, H. & Gao, H. Nanogeochemistry: Geochemical reactions and mass transfers in nanopores. *Geology* **31**, 387–390 (2003).
50. Stack, A. G. Precipitation in Pores: A Geochemical Frontier. *Rev. Mineral. Geochem.* **80**, 165–190 (2015).
51. Jadoon, S. et al. Atom probe tomography and transmission electron microscopy: a powerful combination to characterize the speciation and distribution of Cu in organic matter. *Environ. Sci.: Process. Impacts* **24**, 1228–1242 (2022).
52. Wallander, H., Johansson, L. & Pallon, J. PIXE analysis to estimate the elemental composition of ectomycorrhizal rhizomorphs grown in contact with different minerals in forest soil. *FEMS Microbiol. Ecol.* **39**, 147–156 (2002).
53. Douglas, S. & Beveridge, T. J. Mineral formation by bacteria in natural microbial communities. *FEMS Microbiol. Ecol.* **26**, 79–88 (1998).
54. Durocher, J. L. & Schindler, M. Iron-hydroxide, iron-sulfate and hydrous-silica coatings in acid-mine tailings facilities: A comparative study of their trace-element composition. *Appl. Geochem.* **26**, 1337–1352 (2011).
55. Keshavarzi, M., Davoodi, D., Pourseyedi, S. & Taghizadeh, S. The effects of three types of alfalfa plants (Medicago sativa) on the biosynthesis of gold nanoparticles: an insight into phytomining. *Gold Bulletin* **51**, https://doi.org/10.1007/s13404-018-0237-0 (2018).
56. Thanh, N. T. K., Maclean, N. & Mahiddine, S. Mechanisms of Nucleation and Growth of Nanoparticles in Solution. *Chem. Rev.* **114**, 7610–7630 (2014).
57. Polte, J. Fundamental growth principles of colloidal metal nanoparticles – a new perspective. *CrystEngComm* **17**, 6809–6830 (2015).
58. Neubauer, E., Köhler, S. J., von der Kammer, F., Laudon, H. & Hofmann, T. Effect of pH and stream order on iron and arsenic speciation in boreal catchments. *Environ. Sci. Technol.* **47**, 7120–7128 (2013).
59. Vasyukova, E. V. et al. Trace elements in organic- and iron-rich surficial fluids of the boreal zone: Assessing colloidal forms via dialysis and ultrafiltration. *Geochimica et. Cosmochimica Acta* **74**, 449–468 (2010).
60. Gartman, A. et al. Boiling-induced formation of colloidal gold in black smoker hydrothermal fluids. *Geology* **46**, https://doi.org/10.1130/G39492.1 (2017).
61. Gartman, A. et al. The role of nanoparticles in mediating element deposition and transport at hydrothermal vents. *Geochimica et Cosmochimica Acta* **261**, https://doi.org/10.1016/j.gca.2019.06.045 (2019).
62. Saunders, J. A. Colloidal transport of gold and silica in epithermal precious-metal systems: Evidence from the Sleeper deposit, Nevada. *Geology* **18**, 757–760 (1990).
63. Channell, J. E. T. et al. Biogenic magnetite, detrital hematite, and relative paleointensity in Quaternary sediments from the Southwest Iberian Margin. *Earth Planet. Sci. Lett.* **376**, 99–109 (2013).
64. Robie, R. A. & Bethke, P. M. Molar volumes and densities of minerals. *Rep. No* **822**, 39 (1962).
65. Mansor, M. & Xu, J. Benefits at the nanoscale: a review of nanoparticle-enabled processes favouring microbial growth and functionality. *Environ. Microbiol.* **22**, 3633–3649 (2020).
66. Posfai, M., Buseck, P. R., Bazylinski, D. A. & Frankel, R. B. Iron sulfides from magnetotactic bacteria; structure, composition, and phase transitions. *Am. Mineralogist* **83**, 1469–1481 (1998).
67. Findlay, A. J. Microbial impact on polysulfide dynamics in the environment. *FEMS Microbiol Lett* **363**, https://doi.org/10.1093/femsle/fnw103 (2016).
68. Benzerara, K. et al. Intracellular Ca-carbonate biomineralization is widespread in cyanobacteria. *Proc. Natl Acad. Sci. USA* **111**, 10933–10938 (2014).
69. Fairbrother, L. et al. Supergene gold transformation: Biogenic secondary and nano-particulate gold from arid Australia. *Chem. Geol.* **320-321**, 17–31 (2012).
70. Reith, F. et al. Biological role in the transformation of platinum-group mineral grains. *Nat. Geosci.* **9**, 294–298 (2016).
71. Shammi, M., Pan, X., Mostofa, K. M. G., Zhang, D. & Liu, C.-Q. Photo-flocculation of microbial mat extracellular polymeric substances and their transformation into transparent exopolymer particles: Chemical and spectroscopic evidences. *Sci. Rep.* **7**, 9074 (2017).
72. Costa, O. Y. A., Raaijmakers, J. M. & Kuramae, E. E. Microbial Extracellular Polymeric Substances: Ecological Function and Impact on Soil Aggregation. *Front. Microbiol.* **9** https://doi.org/10.3389/fmicb.2018.01636 (2018).
73. Flemming, H.-C. & Wingender, J. The biofilm matrix. *Nat. Rev. Microbiol.* **8**, 623–633 (2010).
74. Koenigsmark, F. et al. Crystal lattice defects in nanocrystalline metacinnabar in contaminated streambank soils suggest a role for biogenic sulfides in the formation of mercury sulfide phases. *Environ. Sci.: Process. Impacts* **25**, 445–460 (2023).
75. Martin, S. T. Phase Transitions of Aqueous Atmospheric Particles. *Chem. Rev.* **100**, 3403–3454 (2000).
76. Anastasio, C. & Martin, S. T. Atmospheric nanoparticles. *Rev. Mineral. Geochem.* **44**, 293–349 (2001).
77. Donado, E. B. et al. Insights into the mixing of particulate matter and aerosols from different sources in a Caribbean industrial town: composition and possible health effect. *Air Qual., Atmosphere Health* **16**, 1291–1310 (2023).
78. González-Jiménez, J. M. & Reich, M. An overview of the platinum-group element nanoparticles in mantle-hosted chromite deposits. *Ore Geol. Rev.* **81**, 1236–1248 (2017).
79. Baalousha, M. et al. Discovery and potential ramifications of reduced iron-bearing nanoparticles—magnetite, wüstite, and zero-valent iron—in wildland–urban interface fire ashes. *Environ. Sci.: Nano* **9**, 4136–4149 (2022).
80. Silva, L. F. O., Schindler, M., Alavijeh, M. A., Finkelman, R. B. & Oliveira, M. L. S. A review of the mineralogical and chemical composition of nanoparticles associated with coal fires. *J. Environ. Qual.* **51**, 1103–1117 (2022).
81. Bodí, M. B. et al. Wildland fire ash: Production, composition and eco-hydro-geomorphic effects (vol 130, pg 103, 2014). *Earth-Sci. Rev.* **138**, 503–503 (2014).
82. Querol, X. et al. Influence of soil cover on reducing the environmental impact of spontaneous coal combustion in coal waste gobs: A review and new experimental data. *Int. J. Coal Geol.* **85**, 2–22 (2011).
83. Stracher, G. B. & Stracher, G. B. in *Geology of Coal Fires: Case Studies from Around the World* Vol. 18 0 (Geological Society of America, 2007).

84. Reich, M. et al. Formation of cristobalite nanofibers during explosive volcanic eruptions. *Geology* **37**, 435–438 (2009).
85. Larocque, A. C. L. et al. Deposition of a high-sulfidation Au assemblage from a magmatic volatile phase, Volcán Popocatépetl, Mexico. *J. Volcanol. Geotherm. Res.* **170**, 51–60 (2008).
86. Taran, Y. A., Bernard, A., Gavilanes, J.-C. & Africano, F. Native gold in mineral precipitates from high-temperature volcanic gases of Colima volcano, Mexico. *Appl. Geochem.* **15**, 337–346 (2000).
87. Stolzenburg, D. et al. Atmospheric nanoparticle growth. *Rev. Mod. Phys.* **95**, 045002 (2023).
88. Kulmala, M. How particles nucleate and grow. *Science* **302**, 1000–1001 (2003).
89. Eyring, V. et al. *Climate Change 2021: The Physical Science Basis*. *Contribution of Working Group14 I to the Sixth Assessment Report of the Intergovernmental Panel on Climate Change; Chapter Three; Human influence on the climate system*. (2021).
90. Lelieveld, J., Evans, J. S., Fnais, M., Giannadaki, D. & Pozzer, A. The contribution of outdoor air pollution sources to premature mortality on a global scale. *Nature* **525**, 367–371 (2015).
91. Yang, Y. et al. Discovery and ramifications of incidental Magnéli phase generation and release from industrial coal-burning. *Nat. Commun.* **8**, 194 (2017).
92. McDaniel, D. K. et al. Pulmonary Exposure to Magnéli Phase Titanium Suboxides Results in Significant Macrophage Abnormalities and Decreased Lung Function. *Front Immunol.* **10**, 2714 (2019).
93. Guo, Y., Teixeira, J. P. & Ryti, N. Ambient Particulate Air Pollution and Daily Mortality in 652 Cities. *New Engl. J. Med.* **381**, https://doi.org/10.1056/NEJMoa1817364 (2019).
94. Alshehri, T. et al. Wildland-urban interface fire ashes as a major source of incidental nanomaterials. *J. Hazard. Mater.* **443**, 130311 (2022).
95. Aguilera, R., Corringham, T., Gershunov, A. & Benmarhnia, T. Wildfire smoke impacts respiratory health more than fine particles from other sources: observational evidence from Southern California. *Nat. Commun.* **12**, 1493 (2021).
96. Wirth, R., Reid, D. & Schreiber, A. Nanometer-sized platinum-group minerals (PGM) in base metal sulfides: New evidence for an orthomagmatic origin of the Merensky Reef PGE ore deposit, Bushveld Complex, South Africa. *Can. Mineralogist* **51**, 143–155 (2013).
97. Helmy, H. M. et al. Noble metal nanoclusters and nanoparticles precede mineral formation in magmatic sulphide melts. *Nat. Commun.* **4**, 2405 (2013).
98. Junge, M., Wirth, R., Oberthür, T., Melcher, F. & Schreiber, A. Mineralogical siting of platinum-group elements in pentlandite from the Bushveld Complex, South Africa. *Mineralium Depos.* **50**, 41–54 (2014).
99. McLeish, D. F., Williams-Jones, A. E., Vasyukova, O. V., Clark, J. R. & Board, W. S. Colloidal transport and flocculation are the cause of the hyperenrichment of gold in nature. *Proc. Natl Acad. Sci.* **118**, e2100689118 (2021).
100. Duan, H., Wang, C., Hu, R., Zhu, J. & Deng, J. Supernormal enrichment of cadmium in sphalerite via coupled dissolution-reprecipitation process. *Commun. Earth Environ.* **4**, 356 (2023).
101. Masuda, H., Peacor, D. R. & Dong, H. Transmission electron microscopy study of conversion of smectite to illitein mudstones of the Nankai Trough: Contrast with coeval bentonites. *Clays Clay Miner.* **49**, 109–118 (2001).
102. Cho, H. D. & Mermut, A. R. Evidence for Halloysite Formation from Weathering of Ferruginous Chlorite. *Clays Clay Miner.* **40**, 608–619 (1992).
103. Schindler, M. & Hochella, M. F. Sequestration of Pb–Zn–Sb- and As-bearing incidental nanoparticles by mineral surface coatings and mineralized organic matter in soils. *Environ. Sci.: Process. Impacts* **19**, 1016–1027 (2017).
104. González-Jiménez, J. M. et al. Polymetallic nanoparticles in pyrite from massive and stockwork ores of VMS deposits of the Iberian Pyrite Belt. *Ore Geol. Rev.* **145**, 104875 (2022).
105. Hough, R. M., Noble, R. R. P. & Reich, M. Natural gold nanoparticles. *Ore Geol. Rev.* **42**, 55–61 (2011).
106. Cron, B., Macalady, J. L. & Cosmidis, J. Organic Stabilization of Extracellular Elemental Sulfur in a Sulfurovum-Rich Biofilm: A New Role for Extracellular Polymeric Substances? *Front Microbiol* **12**, 720101 (2021).
107. Kennedy, C. B., Scott, S. D. & Ferris, F. G. Characterization of Bacteriogenic Iron Oxide Deposits from Axial Volcano, Juan de Fuca Ridge, Northeast Pacific Ocean. *Geomicrobiol. J.* **20**, 199–214 (2003).
108. Spiro, T. G., Bargar, J. R., Sposito, G. & Tebo, B. M. Bacteriogenic manganese oxides. *Acc. Chem. Res* **43**, 2–9 (2010).
109. Gharieb, M. M., Wilkinson, S. C. & Gadd, G. M. Reduction of selenium oxyanions by unicellular, polymorphic and filamentous fungi: Cellular location of reduced selenium and implications for tolerance. *J. Ind. Microbiol.* **14**, 300–311 (1995).
110. Falciatore, A. & Bowler, C. Revealing the molecular secrets of marine diatoms. *Annu Rev. Plant Biol.* **53**, 109–130 (2002).
111. Rea, I., Terracciano, M. & De Stefano, L. Synthetic vs Natural: Diatoms Bioderived Porous Materials for the Next Generation of Healthcare Nanodevices. *Adv. Healthc Mater.* **6**, https://doi.org/10.1002/adhm.201601125 (2017).
112. Hu, S. Identification of greigite in lake sediments and its magnetic significance. *Sci. China Ser. D.* **45**, 81 (2002).
113. Chang, L. et al. Identification and environmental interpretation of diagenetic and biogenic greigite in sediments: A lesson from the Messinian Black Sea. *Geochem., Geophysics, Geosystems* **15**, 3612–3627 (2014).
114. Moreau, J. W., Webb, R. I. & Banfield, J. F. Ultrastructure, aggregation-state, and crystal growth of biogenic nanocrystalline sphalerite and wurtzite. *Am. Mineralogist* **89**, 950–960 (2004).
115. Madden, A. S. et al. Long-term solid-phase fate of co-precipitated U(VI)-Fe(III) following biological iron reduction by Thermoanaerobacter. **97**, 1641-1652 https://doi.org/10.2138/am.2012.4122 (2012).
116. Suzuki, Y., Kelly, S. D., Kemner, K. M. & Banfield, J. F. Nanometre-size products of uranium bioreduction. *Nature* **419**, 134–134 (2002).
117. Vetriani, C. et al. Mercury adaptation among bacteria from a deep-sea hydrothermal vent. *Appl Environ. Microbiol* **71**, 220–226 (2005).
118. Meeker, K. A., Chuan, R. L., Kyle, P. R. & Palais, J. M. Emission of elemental gold particles from Mount Erebus, Ross Island, Antarctica. *Geophys. Res. Lett.* **18**, 1405–1408 (1991).
119. Baurier Aymat, S. et al. Nanoscale Structure of Zoned Laurites from the Ojén Ultramafic Massif, Southern Spain. *Minerals* **9**, 288 (2019).
120. Jiménez–Franco, A. et al. Nanoscale constraints on the in situ transformation of Ru–Os–Ir sulfides to alloys at low temperature. *Ore Geol. Rev.* **124**, 103640 (2020).
121. Xiong, F. et al. Mineralogical and isotopic peculiarities of high-Cr chromitites: Implications for a mantle convection genesis of the Bulqiza ophiolite. *Lithos* **398-399**, 106305 (2021).
122. Chorover, J., Kretzschmar, R., Garcia-Pichel, F. & Sparks, D. L. Soil Biogeochemical Processes within the Critical Zone. *Elements* **3**, 321–326 (2007).

Acknowledgements

We acknowledge financial support from a NSERC Discovery grant (RGPIN-2023-04726) to MS. JX was supported by the National Science Foundation under Grant No. 2311021 and by the U.S. Department of Energy, Office

of Science, Basic Energy Sciences program under Award Number DE-SC0023251. MH acknowledges support from Virginia Tech's NanoEarth (NSF Award 2025151) and the Office of Faculty Affairs. We thank three anonymous reviewers for their thorough and constructive comments and suggestions.

Author contributions

All authors jointly wrote the paper. MS had the idea for the review, conducted data analysis for the abiotic pathways and wrote the abiotic section. JX compiled the data for the biotic pathways and wrote the biotic section. MH wrote the introduction, and the last section entitled "Overall assessment of Earth NM formation pathways".

Competing interests

The authors declare no competing interests.

Additional information

Supplementary information The online version contains supplementary material available at https://doi.org/10.1038/s43247-024-01823-8.

Correspondence and requests for materials should be addressed to Michael Schindler.

Peer review information *Communications Earth & Environment* thanks the anonymous reviewers for their contribution to the peer review of this work. Primary Handling Editor: Carolina Ortiz Guerrero. A peer review file is available.